

Analytical and Numerical Models of Steel I-Section Beam-Columns Strengthened with Bonded Prestressed FRP Laminates

E.Y. Sayed-Ahmed*

Construction Engineering Dept., the American University in Cairo, Egypt

A.T. Abdelrazik

Civil, Arch. and Env. Engineering Dept., Missouri Univ. of Science & Technology, USA

ABSTRACT: Fibre Reinforced Polymer (FRP) laminate are currently used in strengthening steel structures having a significant favorable effect on the member capacity. Researches have been focused on FRP strengthened beams or columns; thus, I-section beam-columns strengthened with prestressed bonded FRP laminate are scrutinized. Steel yielding, laminate rupture and/or laminate interfacial debonding common failure modes affecting the strengthened beam-columns capacity: debonding commonly leads to a premature failure. Prestressing the FRP laminate may delay this premature failure. Equations are analytically developed to evaluate the interfacial shear and normal stresses between the laminate and the steel; hence, the maximum stresses at debonding are evaluated. Thus, the capacity of a beam-column with prestressed FRP laminate is analytically estimated. A nonlinear numerical model is then developed for these beam-columns. The model is verified against experimental results available from literature. Then, a parametric study is conducted using the numerical model. Based on these results, a regression analysis is performed and the capacity of beam-columns with prestressed FRP laminate is numerically estimated considering steel yielding or FRP laminate rupture. Results of the numerical and analytical models lead to a proposal for evaluating the FRP strengthened beam-column capacity and the need for prestressing the FRP laminate.

1 INTRODUCTION

Fibre Reinforced Polymers (FRP) laminate are currently used in strengthening structural steel members (Teng et al. 2012). However, applications of these new advanced composite materials are almost limited to strengthen steel beams or columns (Liu et al. 2001, Chajes et al. 2003, Donga et al. 2013, Sundarraja et al. 2014, Deng et al. 2016). For example, Denga and Lee (2007) presented an experimental study on steel beams strengthened with bonded CFRP plates. Another two investigations (Chiew et al. 2011a, 2011b) presented a model for predicting the failure load corresponding to debonding of the FRP laminate from the beams. Full-scale bending tests on FRP strengthened steel beams were carried out and then numerical analyses were conducted on these strengthened steel beams. Benachour et al. (2008) presented another theoretical investigation on the interfacial stress between the steel beam and the FRP laminate and compared their results to those developed by Al-Emrani and Kliger (2006). They argued that there is a high concentration of shear and peeling stresses at the ends of the FRP laminate. Generally, FRP laminate adopted in strengthening steel sections are not economically utilized due to the premature interfacial debonding failure (Ghareeb et al. 2013,

Gharib et al. 2015, Gharib et al. 2017, Sayed-Ahmed 2004 and 2006, Teng et al. 2015, Colombi and Fava 2015). In the same time, high strength adhesive will not prevent this mode of failure as the stresses generated in the adhesive layer is always significantly higher than its strength.

Herein, the ultimate capacity of steel I-section beam-columns strengthened by unprestressed or prestressed bonded FRP laminate is scrutinized where prestressing is thought to delay the premature FRP laminate debonding. The investigation starts by analytically developing equations to evaluate the interfacial shear and normal stresses associated with such interfacial debonding. Based on these equations, an expression for the ultimate capacity of beam-columns with bonded unprestressed and prestressed FRP laminate is presented: this expression considers failure by laminate debonding.

Then, a nonlinear numerical model based on the finite element method for the strengthened beam-columns is built-up and verified against previously published experimental investigation. The numerical model is used to evaluate the capacity of the steel beam-columns with bonded FRP laminate and perform a parametric study considering different parameters which are thought to affect the strength of these beam-columns. A regression analysis is performed

using the numerical model data to introduce an equation for the ultimate strength of steel beam-columns with bonded prestressed FRP laminate: the equation considers both the steel yielding and the FRP rupture.

The analytically and numerically developed equations are adopted to introduce a methodology for estimating the ultimate strength and the failure mode of steel beam-columns with bonded FRP laminate. The need for prestressing to delay the FRP laminate debonding is arbitrated using this methodology.

2 THE ANALYTICAL MODEL

Benachour et al. (2008) assumptions are utilized to develop a model for steel beam-columns with bonded FRP laminate. Figure 1a shows a schematic sketch of a beam-column strengthened using a bonded prestressed laminate. The prestressed laminate is attached to the tension flange and has the same length of the beam-column. The beam-column is subjected to constant bending moment and normal force along its span. No end anchorages are applied to the prestressed laminate: prestressing is transferred to the beam-column via bond.

2.1 Interfacial Shear Stress

Referring to Figure1, the interfacial shear stress $\tau(x)$ was introduced as (Abdelrazik 2013):

$$\tau(x) = \frac{G_a}{t_a} [u_l(x) - u_s(x)]$$

Thus,

$$\frac{d^2\tau(x)}{dx^2} = \frac{G_a b_l}{t_a} \left[\frac{1}{A_l E_l} + \frac{1}{A_s E_s} + \frac{h^2}{4E_s I_s} \right] \tau(x) \tag{1}$$

$$= [\lambda^2] \tau(x)$$

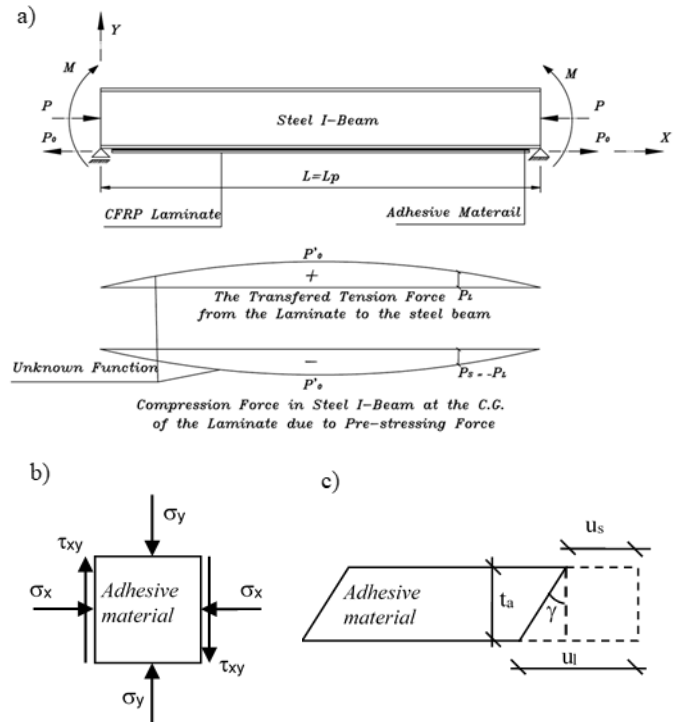


Figure 1 a) Beam-column strengthened with prestressed FRP laminate; b) Shear and normal stress in a prism of the adhesive; c) The adhesive shear strain.

where A_l , b_l , and E_l are the FRP laminate’s cross section area, width and elastic modulus, respectively. A_s , I_s , h , and E_s are the steel beam-column’s cross sectional area, second moment of area, section’s height and modulus of elasticity, respectively. t_a and G_a are the adhesive layer’s thickness and shear modulus, respectively.

The solution of the above second order differential equation is given by

$$\tau(x) = B_1 \cosh(\lambda x) + B_2 \sinh(\lambda x)$$

$$\lambda = \sqrt{\frac{G_a b_l}{t_a} \left[\frac{1}{A_l E_l} + \frac{1}{A_s E_s} + \frac{h^2}{4E_s I_s} \right]} \tag{2}$$

where B_1 and B_2 are arbitrary constants and λ is a properties of the steel section with the bonded FRP laminates.

Two boundary conditions may be written and utilized to find the constants of integration of Eq. (2). The first one requires the interfacial shear stresses at the middle of the FRP laminate to be zero because this point lies on the axis of symmetry. Thus,

$$\text{At } x = l_p / 2 \rightarrow \tau(l_p / 2) = 0 \tag{3a}$$

$$\text{thus, } B_1 = -B_2$$

The second boundary condition implies that at the starting point of the FRP laminate, the compression

force in the steel beam-column due to the prestressing force is equal to zero and the FRP laminate moment contribution is also equal to zero so the steel beam-column's moment contribution has a value equals to the externally acting bending moment. Thus,

$$\text{At } x=0 \rightarrow P_l(0) = P_s(0) = 0 \text{ and } M_s(0) = M \quad (3b)$$

$$\text{thus, } B_2 = \frac{G_a}{\lambda t_a} \left[\frac{P_0}{A_l E_l} - \frac{Mh}{2E_s I_s} + \frac{P}{E_s A_a} \right]$$

where P and M are the external normal force and bending moment, respectively and P_0 is the laminate prestressing force.

Based on Equations 2 and 3, the interfacial shear stress $\tau(x)$ may given by

$$\tau(x) = -B_2 e^{-\lambda x}$$

$$\tau(0) = \frac{G_a}{\lambda t_a} \left[-\frac{P_0}{A_l E_l} + \frac{Mh}{2E_s I_s} - \frac{P}{E_s A_a} \right] \quad (4)$$

2.2 Interfacial Normal Stress

Figure 1b shows a prism element of the adhesive material where $\sigma_n(x) \approx 0$. The interfacial normal stresses σ are defined by Abdelrazik (2013) as

$$\sigma(x) = E_a \varepsilon_a = \frac{E_a}{t_a} [v_l(x) - v_s(x)]$$

thus,

$$\frac{d^4 \sigma(x)}{dx^4} + \frac{E_a}{t_a} \left[D_{11} + \frac{t_l}{E_s I_s} \right] \sigma(x) + \left[\frac{b_l}{2E_s I_s} - \frac{D_{11} t_l}{2} \right] \frac{d\tau(x)}{dx} = 0 \quad (5)$$

where ε_a is the vertical strain in the adhesive material, t_a is the adhesive material's thickness, v_s is the steel beam's lower flange vertical displacement, v_l is the vertical displacement of the bounded prestressed laminate and E_a is the modulus of elasticity of adhesive material.

The solution of this 4th order differential equation is given by

$$\sigma(x) = e^{\beta x} (C_1 \cos \beta x + C_2 \sin \beta x) - n_1 \frac{d\tau(x)}{dx}$$

$$\beta = \sqrt[4]{\frac{E_a}{4t_a} \left[\frac{b_l}{2E_s I_s} - \frac{D_{11} t_l}{2} \right]} \quad (6)$$

$$n_1 = \frac{b_l h - D_{11} E_s I_s t_l}{2(D_{11} E_s I_s + b_l)}$$

$$D_{11} = \frac{12}{t^3 E_l}$$

where C_1 and C_2 are arbitrary constants; D_{11} is the flexural flexibility of the externally bonded prestressed laminate; t_a and E_a are the thickness and the modulus of elasticity of the adhesive layer; and t_l , b_l and E_l are the laminate thickness, width and modulus of elasticity, respectively. In Equation 6, the shear stress $\tau(x)$ is given by Equation 4 while, D_{11} , n_1 and β are properties of the steel section with the bonded FRP laminate.

Two boundary conditions may be written and utilized to find the constants of integration of Equation 6. The first one requires moment contribution at the starting point of the FRP laminate to be zero, so the steel beam-column's moment contribution has a value equals to the externally acting bending moment. The second boundary condition requires both the FRP laminate and steel beam-column's shear contribution to be to zero; this is because the externally acting shear force is equal to zero. Thus, the two boundary conditions may be written as

$$\text{At } x=0$$

$$\rightarrow M_l(0) = 0 \text{ and } M_s(0) = M \quad (7)$$

$$\rightarrow V_l(0) = 0 \text{ and } V_s(0) = V$$

Using on Equation 7, the two constants C_1 and C_2 are given by

$$C_1 = \frac{E_a M}{2\beta^2 E_s I_s t_a} + \frac{n_3 B_2}{2\beta^3} + \frac{n_1 B_2 \lambda^3 (\beta - \lambda)}{2\beta^3}$$

$$C_2 = \frac{-E_a M}{2\beta^2 E_s I_s t_a} - \frac{n_1 B_2 \lambda^3}{2\beta^2} \quad (8)$$

$$n_3 = \frac{E_a}{t_a} \left(\frac{b_l h}{2E_s I_s} - D_{11} \frac{t}{2} \right)$$

Based on Equations 6 and 8, the interfacial normal stresses σ developed at $x = 0$ is given by

$$\sigma(0) = C_1 - n_1 \lambda B_2 \quad (9)$$

where C_1 , n_1 , λ and B_2 are given by Equations 8, 6, 2 and 4, respectively.

2.3 Ultimate Strength of Beam-Columns with Bonded FRP Laminate

The interfacial shear stress causes premature debonding of the FRP laminate from the steel section. Debonding occurs when the maximum interfacial shear stress given by Equation 4 reaches the ultimate shear strength of the adhesive material; i.e.

$$\tau_{\max} = \frac{G_a}{\lambda \cdot t_a} \left[-\frac{P_0}{A_l E_l} + \frac{Mh}{2E_s I_s} - \frac{P}{E_s A_a} \right] \quad (10)$$

where τ_{\max} is the interfacial shear strength of the adhesive materials.

External acting bending moment M can be written as $P \cdot e$ where P is the external acting normal force and e is the eccentricity of this external acting normal force from the beam-column cross section centroid.

At debonding, with no laminate prestressing, the external load reaches $P_{\max 1}$ where

$$\tau_{\max} = \frac{G_a}{\lambda \cdot t_a} \left[-0 + \frac{P_{\max 1} e h}{2E_s I_s} - \frac{P_{\max 1}}{E_s A_a} \right] \quad (11)$$

Thus, the maximum failure load $P_{\max 1}$ that can be supported by a beam-column with bonded FRP unprestressed laminate with no premature debonding failure may be given by

$$P_{\max 1} \left(\frac{e}{h} - \frac{e_{\min}}{h} \right) = \frac{2\tau_{\max} \lambda t_a E_s I_s}{h^2 G_a} \quad (12)$$

$$\text{where: } e_{\min} = \frac{2I_s}{hA_s}$$

When $e < e_{\min}$, the FRP laminate is will be subjected to compression, so $P_{\max 1}$ has a value that tends to infinity; i.e. no need for strengthening using the FRP laminate.

For prestressing the FRP laminate, the maximum initial prestressing force in the laminate preventing the premature debonding failure (i.e. at zero values for P and M) is using Equation 10 as

$$\begin{aligned} \tau_{\max} &= \frac{G_a}{\lambda \cdot t_a} \left[-\frac{P_{0\max}}{A_l E_l} + 0 + 0 \right] \\ \rightarrow P_{0\max} &= \frac{\tau_{\max} \cdot \lambda \cdot t_a \cdot A_l \cdot E_l}{G_a} \end{aligned} \quad (13)$$

When the laminate is prestressed, the external load reaches $P_{\max 2}$ at debonding of the FRP laminate where

$$\begin{aligned} \tau_{\max} &= \frac{G_a}{\lambda \cdot t_a} \left[-\frac{P_o}{A_l E_l} + \frac{P_{\max 2} e h}{2E_s I_s} - \frac{P_{\max 2}}{E_s A_a} \right] \\ &= \frac{G_a}{\lambda \cdot t_a} \left[-\frac{\tau_{\max} \lambda t_a A_l E_l}{G_a A_l E_l} + \frac{P_{\max 2} e h}{2E_s I_s} - \frac{P_{\max 2}}{E_s A_a} \right] \end{aligned} \quad (14)$$

Thus, the maximum failure load $P_{\max 2}$ which can be supported by a beam-column with bonded FRP prestressed laminate with no premature debonding failure may be given by

$$P_{\max 2} \left(\frac{e}{h} - \frac{e_{\min}}{h} \right) = \frac{4\tau_{\max} \lambda t_a E_s I_s}{h^2 G_a} \quad (15)$$

$$\text{where: } e_{\min} = \frac{2I_s}{hA_s}$$

If the load increases beyond $P_{\max 1}$ or $P_{\max 2}$, premature debonding failure is encountered as the shear stress in the laminate will exceed its ultimate strength.

In Figure 2 and based on the previous equations for $P_{\max 1}$ and $P_{\max 2}$, three curves are schematically plotted. The first curve presents the beam-column eccentric axial load capacity P_u in case of no premature debonding failure; in other words, this beam-column fails by steel yielding or FRP laminate rupture; P_u will be defined for steel beam-columns with bonded prestressed and unprestressed FRP laminate in the next sections. The second curve presents the load causing premature debonding failure $P_{\max 1}$ for steel beam-column with bonded unprestressed FRP laminate. The third curve presents the load causing premature debonding failure $P_{\max 2}$ for steel beam-column with bonded prestressed FRP laminates, which is prestressed to the maximum value of the prestressing force. As shown in Figure 2, P_u curve is divided at the intersection points with $P_{\max 1}$ and $P_{\max 2}$ curves and with the vertical line presenting e_{\min} into four zone as follow:

- Zone L1: no need for strengthening using FRP laminate.

- Zone L2: no premature failure is encountered and no need for prestressing the FRP laminate.
- Zone L3: no premature failure is encountered if the laminate is prestressed below P_{0max} .
- Zone L4: premature failure will take place even if the FRP laminate is prestressed with P_{0max} .

P_{0max} is the maximum initial prestressing force that can be applied to the FRP laminate without debonding from the steel beam-column.

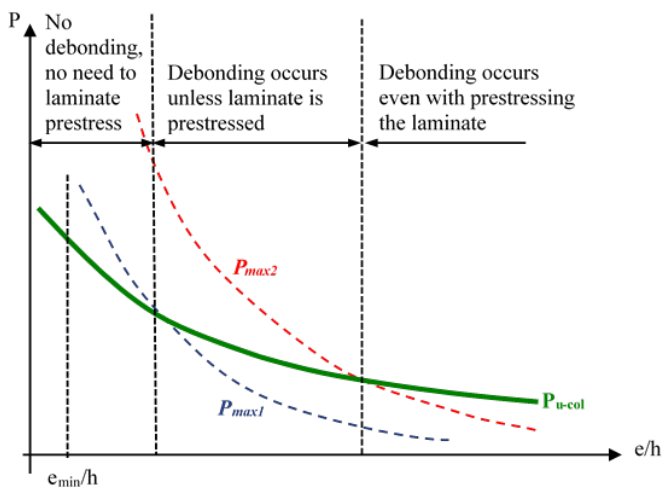


Figure 2 Schematic strength and failure modes of beam-columns with bonded FRP laminates.

3 THE NUMERICAL MODEL

Steel I-section beam-columns with bonded prestressed or unprestressed FRP are numerically simulated using nonlinear finite element models (Figure 3): 8-node shell elements are adopted to model the flanges and web of the I-section as well as the FRP laminates, while 20-node solid elements are used to model the adhesive layer. After testing multiple models, fine mesh of 10 mm element size is used in modeling the FRP laminate, the adhesive, the lower flange of the steel beam and the lower part of the steel web, while a 25 mm element size is used in modeling of the rest of web and the upper flange of the steel I-section.

Full contact is assumed between the adhesive material and the steel flange or the FRP laminate. Thus, debonding failure is encountered when stresses in the interfacial material reaches its strength: strength of the interface between the adhesive and the steel or the FRP is almost equal to the adhesive material strength.

The adopted load model is shown schematically in Figure 4.

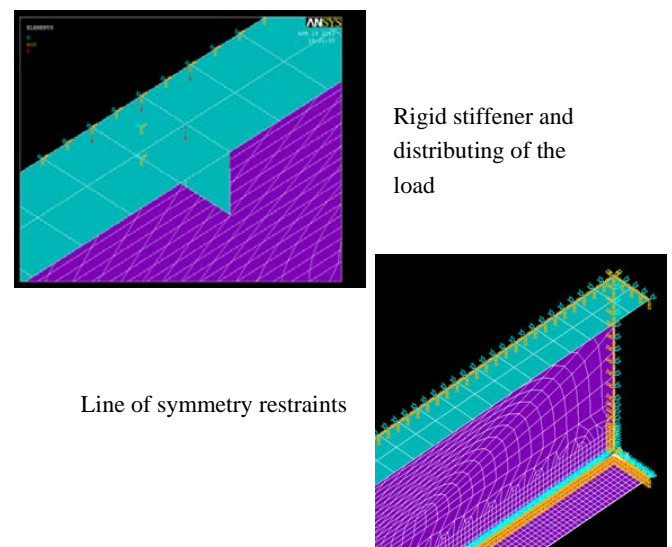
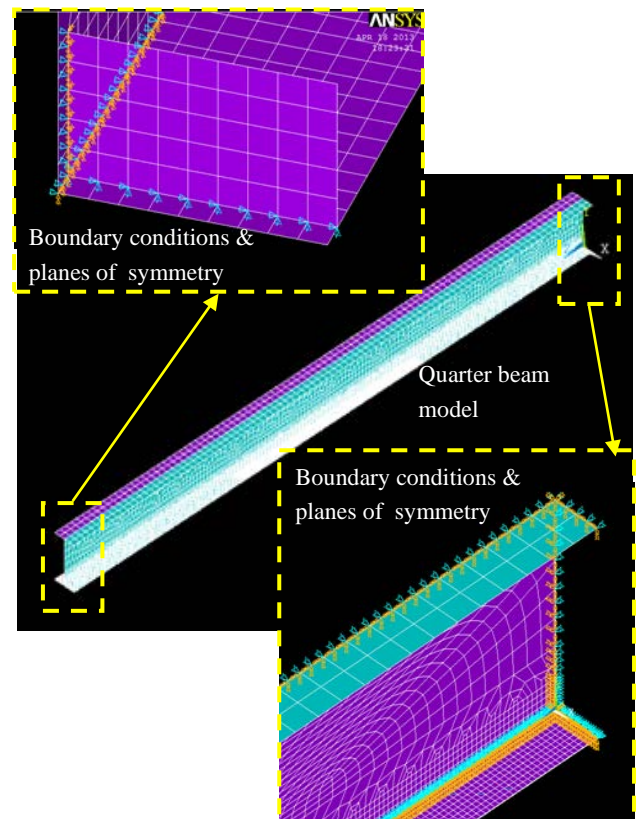
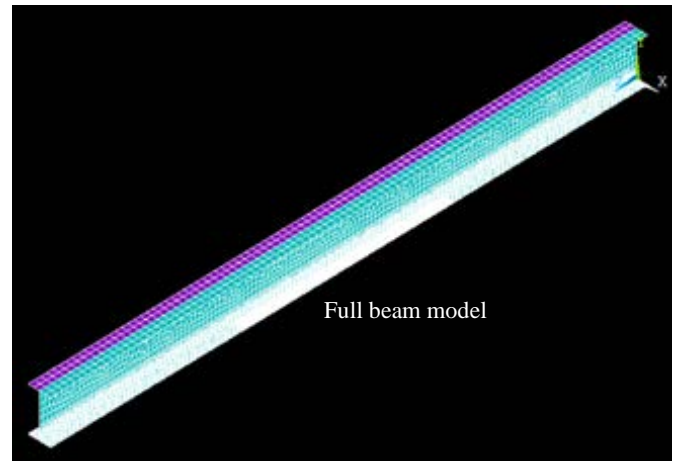


Figure 3 Proposed finite element model of the steel beam-columns.

3.1 Verification of the numerical model results

The model accuracy is validated by comparing its results to previously obtained experimental results (Denga and Lee 2007, Chiew et al. 2011a,b). Full details of the model and its verification are given elsewhere (Abdelrazik 2013) with a summary of the verification analysis presented herein.

Three beams (Beams 1, 2 and 3) were tested in 4-points flexural loading by Chiew et al. (2011a,b). These beams are simulated using the proposed numerical model via ANSYS software. In order to avoid web crippling rigid stiffener are assigned below the loading point. The concentrated load is distributed into five concentrated loads around this stiffener as shown in Figure 3. The stiffeners have a width equal to the flange width and a depth equal to its width; a thick stiffener is chosen in order to uniformly distribute the concentrated loads. In order to avoid the flange local failure the hinged support is assigned as a line support along the flange nodes, a stiffener is also assigned above this line support as shown in Figure 3. Beam 1 was fully modeled, then a quarter beam is modeled and the appropriate restrains are assigned along the planes symmetry: a difference of only 3.8% in the failure loads between the two models is recorded. Thus, Beam 2 and Beam 3 are modeled using a quarter-beam model.

Table 1 summarizes the details of geometric and material properties of the modelled beam. The table also compares the failure load and failure mode recorded experimentally and obtained numerically. The model-predicted failure loads well agree with the experimental investigation's outcomes.

Table 1. Tested beams (Denga and Lee 2007) numerically simulated using the proposed finite element model.

Property		Beam 1	Beam 2	Beams 3
Steel section dim. (mm)	Web	119×4	159×5	159×5
	Flange	76×8	90×8	90×8
Steel section mechanical properties (MPa)	Yield stress	275	334	334
	Elastic modulus	205	192	192
Adhesive thickness (mm)	Thickness	1.0	0.5	0.5
Adhesive mechanical properties (MPa)	Ult. strength	29.7	15.5	15.5
	Elastic modulus	8000	390	390
Laminate dim. (mm)	Length × width × Thickness	400×76×3.0	850×90×1.5	1450×90×1.5
Laminate mechanical properties (MPa)	Ult. Strength	800	800	800
	Elastic modulus	212	212	212
Span (mm)		1100	2400	2400
Load spacing (mm)		300	800	800
Experimental Failure load (kN) and mode	Failure load	127.7	127.4	140.8
	Failure mode	Debonding	Debonding	Yielding
Numerical failure load (kN) and mode	Failure load	125.3	126.4	155.5
	Failure mode	Debonding	Debonding	Yielding
% of diff between experimental and numerical failure load		-1.95%	-0.8%	10%

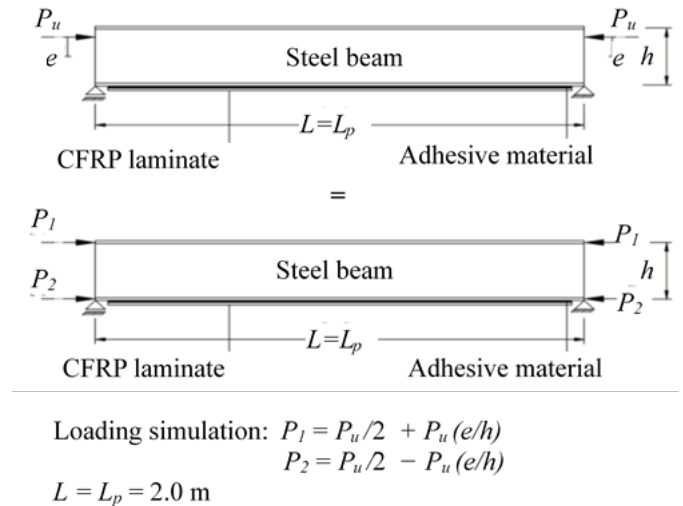


Figure 4. Load model adopted in the numerical modelling.

3.2 Parametric Study

The numerical model is now adopted to investigate the effects of five parameters on the ultimate capacity of beam-column with bonded FRP laminate are investigated. These parameters are the prestressing force P_0 , the axial load eccentricity e , the FRP laminate axial stiffness $E_L A_L$, the steel beam-column depth h , and the steel beam-column flexure stiffness $E_s I_s$.

Each parameter is changed separately in the numerical analysis while the rest of the parameters are kept at the constant values shown in Table 2. The investigated range for the said five parameters are as follow:

- The prestressing force P_0 is considered as 0.0, $0.3P_{0max}$, $0.5P_{0max}$, and $0.7P_{0max}$ where P_{0max} is the maximum prestressing force that can be applied to the FRP laminate without debonding from the steel beam-column.
- The axial load eccentricity-to-depth ratio e/h is taken as 0.5, 1.0, 2.0, 3.0 and 5.0.
- The FRP laminate axial stiffness $E_L A_L$ was based on the number of laminate layers where 1, 2 and 3 layers are considered with laminate thickness of 1.4 mm, 2.8 mm and 4.2 mm. These values correspond to axial stiffness of

3.8×10^4 kN, 7.6×10^4 kN and 11.4×10^4 kN, respectively.

- The steel beam-column depth h is varied between 200 mm and 400 mm keeping a constant flexural stiffness $E_s I_s$ of 15×10^9 kN·mm² by adjusting the beam-column flange thickness.
- The steel beam-column flexure stiffness $E_s I_s$ is varied between 8.4×10^9 kN·mm² to 17.7×10^9 kN·mm² keeping a constant beam-column height of 300 mm and changing the flange thickness to reflect this variation.

Table 2. Data commonly adopted in the parametric study when a parameter is not changed.

F_y MPa	E_s GPa	E_l GPa	E_a MPa	τ_{max} MPa	t_a mm	L mm	h mm	t_f mm	t_l mm	e/h	P_o/P_{0max}
240	192	150.8	390	8.95	1.0	2000	300	12	2.8	3	0.5

As shown in Table 3, a total of 126 models is needed to perform the parametric study covering the above mentioned five parameters. The beam models previously developed for the verification of the numerical analysis results is adjusted herein to the beam-column loading, which is an eccentric normal force, and the beam-column's boundary conditions. The eccentric normal force is divided into two concentrated loads (P_1 and P_2) one at each flange (Figure 4) where

$$P_1 = \frac{P_u}{2} + P_u \frac{e}{h} \quad \text{and} \quad P_2 = \frac{P_u}{2} - P_u \frac{e}{h} \quad (16)$$

Table 3. Numbers of models required to analyze the required five parameters.

	P_0	e/h	$E_L A_L$	$E_s I_s$	h	No. of models
P_0	--	$4 \times 4 = 1$	$4 \times 3 = 1$	$4 \times 4 = 1$	$4 \times 3 = 1$	56
e/h	--	6	2	6	2	40
$E_L A_L$	--	$4 \times 3 = 1$	2	6	2	21
$E_s I_s$	--	$4 \times 3 = 1$	--	2	$3 \times 3 = 9$	9
H	--	--	--	--	--	--
Total no. of models						126

Full contact is assumed between the steel beam-column flange and the adhesive material and also between FRP and the adhesive material; i.e. no contact element is applied as the strength of the interface between the steel and the adhesive material and/or between the adhesive and the FRP laminate is almost equal to the strength of the adhesive itself.

The parametric study outcomes are presented in the form of graphs, and then the 126 models results are

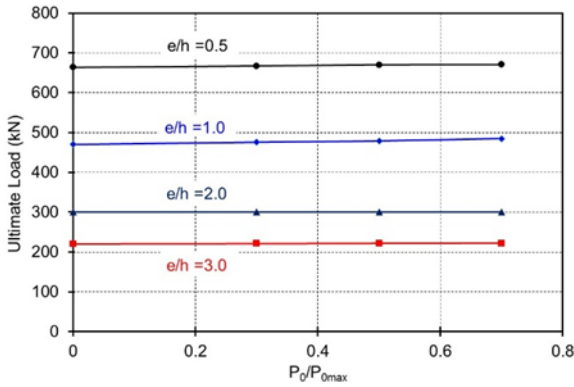
used to form an equation to estimate the load capacity of the beam-column as a function of these parameters considering only the steel yielding failure criteria; the capacity is shown as the P_u curve of Figure 2.

3.3 Results of the Numerical analysis

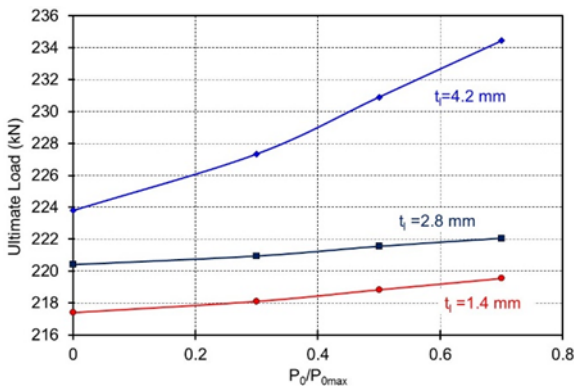
Figure 5 shows the effect of changing the prestressing force on the ultimate load of the beam-column for different eccentricity-to-depth ratio, laminate stiffness, beam-column stiffness and beam-column depth. It is evident from Figure 5a that changing the prestressing force for the same e/h ratio has no significant effect on the value of the ultimate load, while changing the e/h for any value of the prestressing force has a significant effect on the beam-column's ultimate load. Figure 5b also reveals that changing the prestressing force has no significant effect on the beam-column's ultimate load for low values of the laminate stiffness, while it has a higher effect for high values of the laminate stiffness. Figure 5c indicates that changing the prestressing force for the same beam-column stiffness has no significant effect on the beam-column's ultimate load, while the change in the beam-column stiffness caused significant change in the beam-column ultimate load for any value of the prestressing force. Finally, Figure 5d shows that changing the prestressing force for the same beam-column depths has no significant effect in the changing the value of the ultimate load.

Thus, with the exception of very thick FRP laminate, the change in the level of laminate prestressing has no significant effect in changing the value of the beam-column's ultimate load. In other words, laminate prestressing level has no significant effect on the

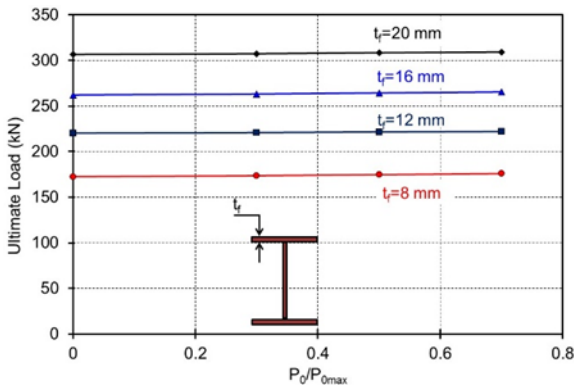
beam-column ultimate load when considering only the yield failure criteria of the beam-column.



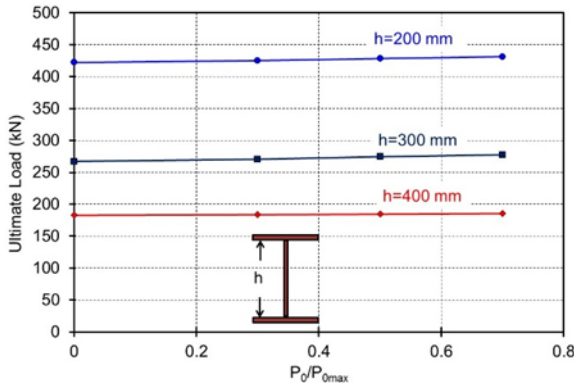
a. Prestressing force and various e/h ratio.



b. Prestressing force and various laminate stiffness.

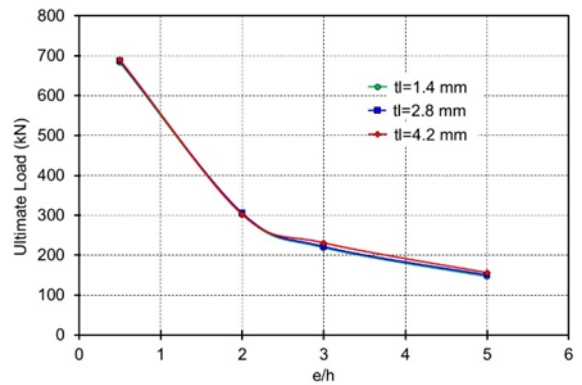


c. Prestressing force and different column stiffness.

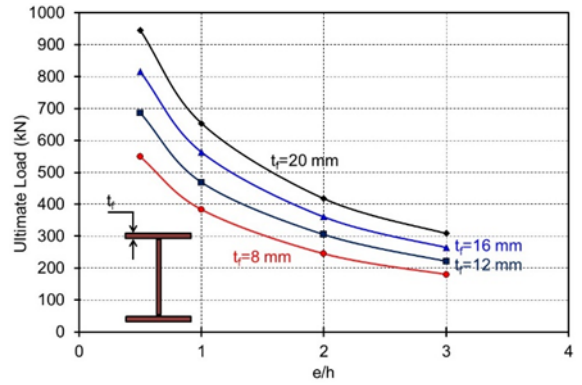


d. Prestressing force and different column depth.

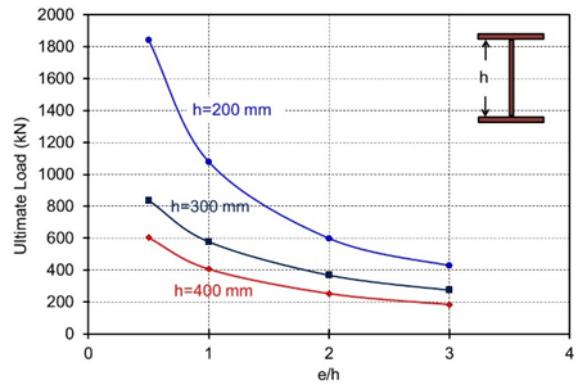
The effect of changing e/h on the beam-column ultimate load is shown in Figure 6 for different laminate stiffness, beam-column stiffness and beam-column depth. The figure reveals that laminate stiffness has a no effect on the beam-column ultimate load for e/h ratios less than 2; while it has a small effect on this load e/h ratios greater than 2. On the other hand, the figure shows that e/h ratio has a pronounced effect on the beam-column's ultimate load for any value for the laminate stiffness. The figure shows the logical effect of both the beam-column stiffness and depth on the ultimate beam-column load.



a. e/h ratio and different laminate stiffness



b. e/h ratio and different beam-column stiffness

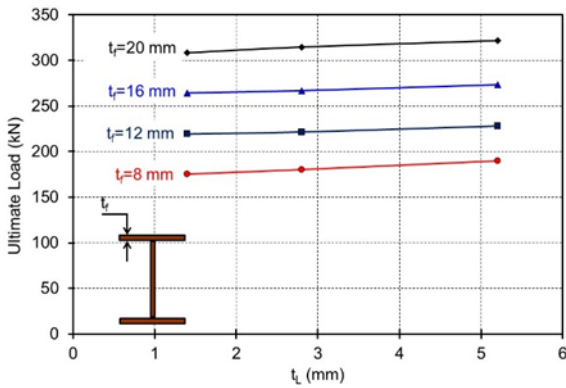


c. e/h ratio and different beam-column depth

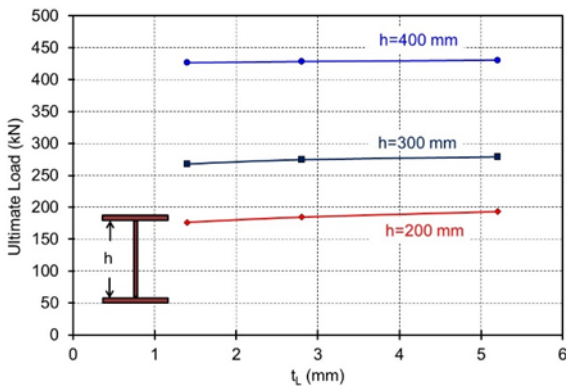
Figure 5. Effect of FRP prestressing level on the beam-column ultimate load.

Figure 6. Effect of eccentricity-to-depth ratio on the beam-column ultimate load.

Figure 7 shows the effect of changing the laminates stiffness for different beam-column stiffness and beam-column depth on the ultimate beam-column's load. Figure 7a indicates that changing the laminate stiffness is more noticeable for beam-columns with small flanges (lower beam-column stiffness) compared to beam-columns with heavier flanges (larger beam-column stiffness). Figure 7b also indicates that the effect of laminate stiffness on the beam-column ultimate capacity is more noticeable for beam-columns with small depths compared to its effect on deeper beam-columns. It is evident from Figure 7 that laminates stiffness has no significant effect on the beam-column ultimate load when considering only the yield failure criteria of the beam-column.



a. Laminate stiffness and different column stiffness



b. Laminate stiffness and different column depth

Figure 7. Effect of laminates stiffness the beam-column ultimate load.

Figure 8 shows the effect of the beam-column stiffness on the ultimate load. It indicates that variation of any of the depth of the beam-column or the stiffness of the beam-column have a significant effect on the beam-column's ultimate load.

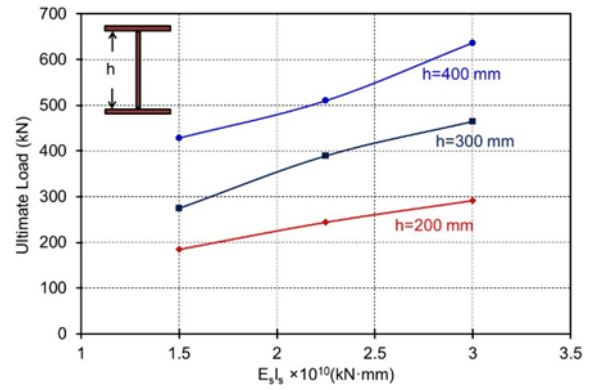


Figure 8. Effect of beam-column stiffness the ultimate load

4 ULTIMATE STRENGTH OF BEAM-COLUMNS WITH BONDED FRP LAMINATE

The numerical analysis results are used to develop an equation for estimating the ultimate load P_u corresponding to either yielding of the steel beam-column or rupture of the FRP laminate assuming no premature debonding failure. The effect of prestressing force variation is ignored as it has minor effect on the ultimate load value in this case. The proposed equation is given by

$$P_u = A_s F_y e^{[\omega_1 + \omega_2 - \omega_3]}$$

$$\omega_1 = 0.00054 \frac{E_s I_s}{A_s F_y h^2}$$

$$\omega_2 = 0.00085 \frac{A_L E_L}{A_s F_y}$$

$$\omega_3 = 0.458 \frac{e}{h} + 0.1829$$
(17)

where, e is the load eccentricity from the steel beam-column section centroid, h is the steel section's depth, E_s is the modulus of elasticity of the steel, I_s is the second moment of area of the beam-column cross section, A_s is the area and of the beam-column's cross section, A_L is the cross sectional area of the FRP laminate, and E_L is the modulus of elasticity of the FRP laminate material.

Equation 17 has a 0.965 correlation coefficient with the numerically obtained ultimate loads. A sample of the comparisons between the ultimate loads numerically obtained using the finite element model and those calculated using Equation 17 is shown in Table 4.

Thus, the capacity of a beam-column strengthened with bonded prestressed FRP laminate can be

calculated as the minimum value of P_u and P_{max} where P_u is given by Equation 17 and P_{max} is defined by

$$P_{max} = P_{max1} + P_0 \quad (18)$$

where P_{max1} is defined by Equation 12 and P_0 is the prestressing force in the FRP laminate which has a maximum value of P_{0max} defined by Equation 13.

Recalling that Equations 12 and 15 results P_{max1} and P_{max2} , which are the ultimate load for beam-columns with unprestressed or prestressed FRP laminates without debonding. Thus, the need for FRP laminate prestressing is defined by the relation between P_u , P_{max1} and P_{max2} (Figure 2) as discussed earlier.

5 FAILURE MODES OF FRP STRENGTHENED BEAM-COLUMN

The beam-column's ultimate load is calculated using Equations 12, 15 and 17 for different load eccentricities and adhesive properties. The load causing yielding failure criteria is not affected by the adhesive properties, while the load causing FRP laminate debonding is affected by both the load eccentricity-to-depth ratio and the adhesive layer properties.

Table 5 shows the data used to calculate P_{max1} , P_{max2} , P_u , M_{max1} , M_{max2} and M_u for different adhesive thicknesses where,

P_u is the eccentric normal force causing failure of the FRP strengthened beam-column by yielding,

P_{max1} is the maximum load sustained by the unprestressed FRP strengthened beam-column before debonding of the FRP laminate,

P_{max2} is the maximum load sustained by prestressed FRP strengthened beam-column before debonding of the FRP laminate,

M_u is value of the two equal and opposite bending moments causing failure of the FRP-strengthened beam-column by yielding,

M_{max1} is the maximum value of the two equal and opposite bending moments sustained by unprestressed FRP strengthened beam-column before debonding of the FRP laminate, and

M_{max2} is the maximum value of the two equal and opposite bending moments sustained by prestressed FRP strengthened beam-column before debonding of the FRP laminate.

The ultimate loads and moments for different eccentricities are determined for adhesive layer thicknesses of 1.0 mm, 0.5 mm and 0.25 mm with the parameters shown in Table 5 and plotted in Figures 9-11.

Table 4. Comparison between the load numerically obtained using the FEM and that is calculated using the proposed equation.

Model no	FRP Prestressing level	$A_s F_y$ (kN)	$(E_s I_s)/(A_s F_y h^2)$	$(A_L E_L)/(A_s F_y)$	e/h	P_{u-FEM} (kN)	$P_{u-Eq 17}$ (kN)	Error %
1	0.0	878.4	145.36	43.26	0.50	663.50	652.89	-1.60
2	$0.3P_{0max}$	878.4	145.36	43.26	0.50	667.22	652.89	-2.15
3	$0.5P_{0max}$	878.4	145.36	43.26	0.50	670.24	652.89	-2.59
4	$0.7P_{0max}$	878.4	145.36	43.26	0.50	670.26	652.89	-2.59
5	0.0	788.75	118.86	48.18	3.00	182.82	184.68	1.02
6	$0.3P_{0max}$	788.75	118.86	48.18	3.00	183.71	184.68	0.53
7	$0.5P_{0max}$	788.75	118.86	48.18	3.00	184.59	184.68	0.05
8	$0.7P_{0max}$	788.75	118.86	48.18	3.00	185.48	184.68	-0.43

Table 5: Data used for estimating the ultimate loads and moment for different adhesive thicknesses

F_y MPa	E_s GPa	E_L GPa	E_a GPa	t_a mm	τ_{max} MPa	h mm	L mm	t_f mm	t_L mm	e/h	P_0/P_{max}
240	192	150.8	390	var.	8.95	300	2000	12	2.8	3	0 or 1

For a 1.0 mm adhesive layer thickness, Figure 9a shows that the P_u , P_{max1} , and P_{max2} are significantly affected by the variation of the e/h ratio; P_u is greater than the values of P_{max1} , and P_{max2} for large e/h ratio. Similarly, Figure 9b, shows that the values of M_u , M_{max1} , and M_{max2} and are also affected by the variation of e/h ratio. Both Figures 9a and 9b define three distinct zones of behaviour:

- Zone 1: $0 < e/h < 1.7$ where $M_u < M_{max1} < M_{max2}$ indicating that the failure in this range of e/h occurs by steel yielding and thus, no need for

prestressing the FRP laminate (the same is valid for P_u , P_{max1} and P_{max2}).

- Zone 2: $1.7 < e/h < 3.8$ where $M_{max2} > M_u > M_{max1}$ indicating that the failure in this range of e/h occurs by either steel yielding or FRP laminate debonding depending on the value of the laminate prestressing force; thus, adequate prestressing level may prevent the premature laminate debonding.
- Zone 3: for $e/h > 3.8$ (large eccentricity simulating beam behaviour) where the value of $M_u > M_{max2} < M_{max1}$ indicating that the FRP laminate

debonding always governs the failure mode even when using the max prestressing force.

12 define Zone 1 in which no FRP prestressing is required where failure will be dominated by steel yielding, Zone 2 in which adequate prestressing of the FRP laminate will serve to avoid FRP laminate debonding and thus failure can occur by steel yielding and Zone 3 in which failure will always occur by FRP laminate debonding even if the FRP laminate is prestressed.

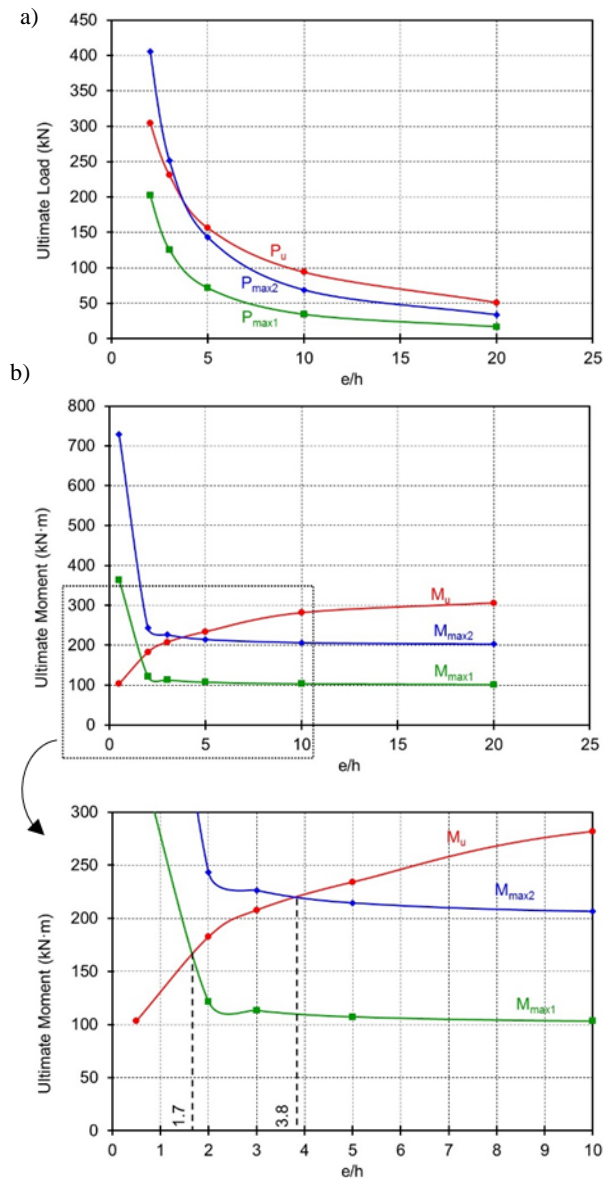


Figure 9. Ultimate load and moment for different e/h ratios and adhesive layer thickness of 1.0 mm.

For adhesive layer thicknesses of 0.5 mm and 0.25 mm, Figures 10 and 11 show similar behaviour to that mentioned above for the 1.0 mm adhesive thickness except that the e/h limits defining the three zones are 1.35 and 1.95 for 0.5 mm adhesive layer thickness and 1.08 and 1.68 for 0.25 mm thickness.

Figures 9 to 11 indicate that the adhesive thickness has minor effect on the ultimate load causing steel yielding P_u , while it has a significant effect on the ultimate load causing debonding for both cases of the prestressed and unprestressed FRP laminate; P_{max1} and P_{max2} , respectively.

The three zones of behaviour defined earlier are also plotted in Figure 12 against the e/h ratio and the adhesive layer thickness t_a . The two curves of Figure

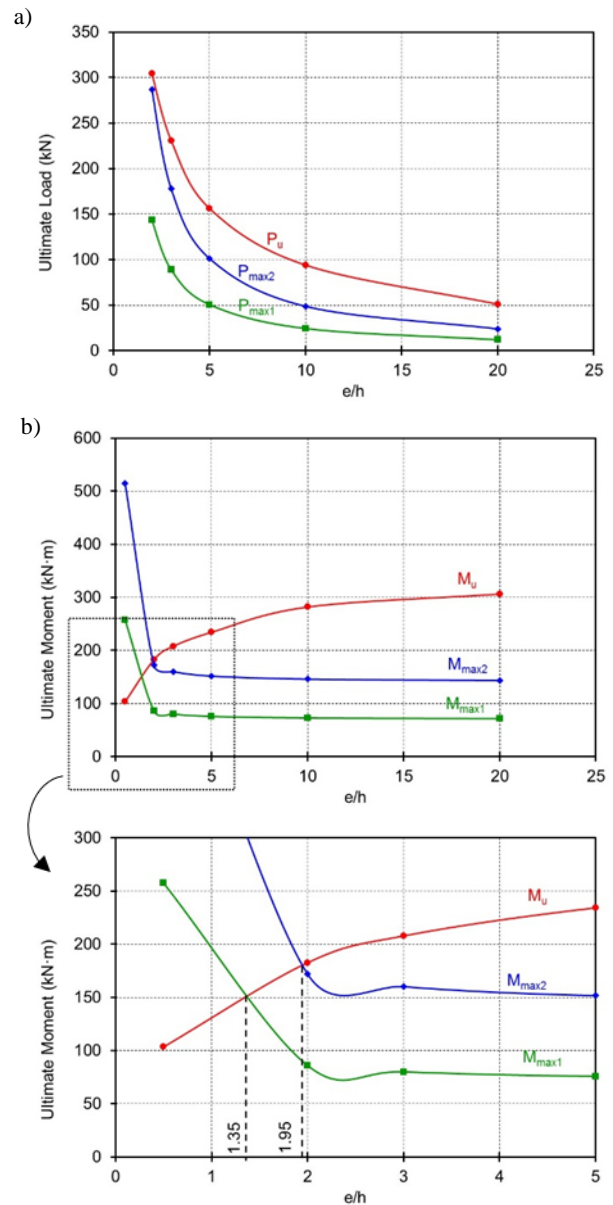


Figure 10. Ultimate load and moment for different e/h ratios and adhesive layer thickness of 0.5 mm.

6 CONCLUSIONS

The ultimate strength of a beam-column with bonded prestressed FRP laminate has been scrutinized. The investigation took two parallel paths:

- First, a closed form solution was developed to estimate the actual interfacial shear and normal stresses in the adhesive layer. Using these stresses, an equation was analytically developed to estimate the ultimate load causing debonding of the FRP laminate from the steel beam-column.

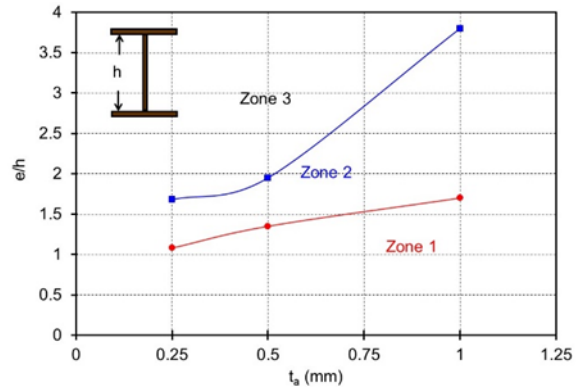


Figure 13. Relation between the eccentricity, the adhesive layer thickness and the three zones defining the failure mode of beam-columns with bonded FRP laminate.

- Then, a numerical model was built-up in order to estimate the ultimate load causing steel yielding of the beam-column. The developed finite element model results were verified using previously published experimental data. Using the finite element model data and performing a regression analysis, another equation is numerically developed to estimate the ultimate load causing steel yielding of the beam-column.

Based on the two equations, a methodology is proposed to determine ultimate capacity of beam-columns strengthened with FRP prestressed laminate where the minimum load resulting from the two equations control the ultimate capacity of the FRP strengthened beam-column. This methodology also defines the failure mode and the need for FRP prestressing.

The analyses shows that strengthening small eccentricity-to-depth ratio beam-columns using FRP laminate has minor effect in raising their ultimate load; this technique is significant in delaying the laminate debonding for larger eccentricity-to-depth ratio and, thus, increasing the beam-column's capacity. Furthermore, beam-columns with small eccentricity-to-depth ratio reach steel yielding before experiencing debonding of the FRP laminate. On the other hand, failure of beam-columns with very large eccentricity-to-depth ratio is always controlled by premature debonding failure of the FRP laminate even when they are prestressed.

The investigation also confirms that both the FRP laminate prestressing and the mechanical properties of the adhesive layer does not affect the ultimate load causing yielding but it has a significant effect on delaying the premature debonding of the laminate from the steel section.

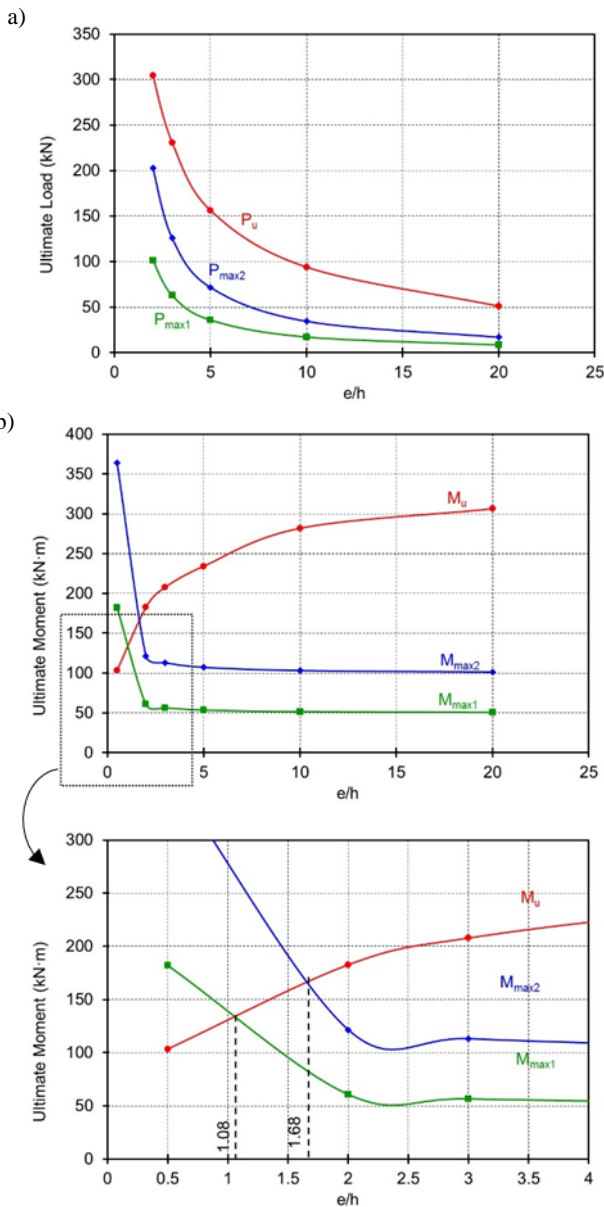


Figure 11. Ultimate load and moment for different e/h ratios and adhesive layer thickness of 0.25 mm.

7 REFERENCES

- Abdelrazik, A. T. Strengthening of Steel I-Section Beam-Column using Prestressed CFRP Laminate. MSc thesis, Ain Shams University Faculty of Engineering, 2013, 154p.
- Al-Emrani, M., Kliger, R. Analysis of interfacial shear stresses in beams strengthened with bonded prestressed laminate. *Journal of Composites Part B*, 2006, 37(4): 265-272.
- Benachour, A., Benyoucef, S., Tounsi, A., AddaBedia, E. Interfacial stress analysis of steel beams reinforced with bonded pre-stressed FRP plate. *Engineering Structures*, 2008, 30(11): 3305-3315.
- Chajes, M., Swinehart, M., Richardson, D., Wenczel, G. Bridge rehabilitation Using advanced composites: Ashland Bridge SR-82 over Red Clay Creek. Proceedings, 10th International Conference and Exhibition-Structural Faults and Repair Conference, London, July 2003 – CD Rom.
- Chiew, S., Yu, Y., Lee, C. Bond failure of steel beams strengthened with FRP laminate - Part 1: Model development. *Journal of Composites Part B*, 2011a, 42(5): pp.1114-1121.
- Chiew, S., Yu, Y., Lee, C. Bond failure of steel beams strengthened with FRP laminate - Part 2: Verification. *Journal of Composites Part B: Engineering*, 2011b, 42(5): pp.1122-1134.
- Colombi, P., Fava, G. Experimental study on the fatigue behaviour of cracked steel beams repaired with CFRP plates. *Engineering Fracture Mechanics*, 2015, 145: 128-142.
- Deng, J., Jia, Y., Zheng, H. Theoretical and experimental study on notched steel beams strengthened with CFRP plate. *Composite Structures*, 2016, 136: pp. 450-459
- Denga, J., Lee, M. Behaviour under static loading of metallic beams reinforced with a bonded CFRP plate. *Composite Structures*, 2007, 78(2): pp. 232-242.
- Donga, J.F., Wang, Q.Y., Guanb, Z.W. Structural behaviour of recycled aggregate concrete filled steel tube columns strengthened by CFRP. 2013, *Engineering Structures*, 48: pp. 532-542
- Ghareeb, M., Khadr, M., Sayed-Ahmed, E. CFRP Strengthening of Steel I-Beam against Local Web Buckling: a Numerical Analysis. 2013, Proceedings, 5th International Conference on Structural Engineering, Mechanics and Computation, Cape Town, South Africa, 2013, pp. 2421-2425.
- Gharib, M.A., Khushefati, W.H., Khedr, M.A., Sayed-Ahmed, E.Y. Performance of steel beams strengthened with prestressed CFRP laminate. *Electronic Journal of Structural Engineering*, 2015, 15: 60-69,.
- Gharib, M.A., Khushefati, W.H., Khedr, M.A., Sayed-Ahmed, E.Y. Steel beams strengthened with prestressed CFRP laminate: is there a need for laminate prestressing? *Electronic Journal of Structural Engineering*, 2016, 16 (1): 53-63.
- Liu, X., Silva, P., Nanni, A. Rehabilitation of steel bridge members with FRP composite materials. Proceedings, Composite in Construction, Portugal, 2001, pp. 613-617
- Sayed-Ahmed, E. Strengthening of Thin-Walled Steel I-Section Beams Using CFRP Strips, Proceedings, 4th International Conference on Advanced Composite Materials in Bridges and Structures, Calgary, Canada, 2004.
- Sayed-Ahmed, E. Numerical Investigation into Strengthening Steel I-Section Beams Using CFRP Strips. Proceedings, 6th Structures Congress, ASCE, St. Louis, USA, 2006, pp. 1-8.
- Sundararaja, M.C., Sriram, P., Ganesh Prabhu, G. Strengthening of Hollow Square Sections under Compression Using FRP Composites”. *Advances in Materials Science and Engineering*, 2014, 19p.
- Teng, J.G., Fernando, D. Strengthening of steel structures with fiber-reinforced polymer composites. *Journal of Constructional Steel Research*, 2012, 78: pp. 131-143.
- Teng, J.G., Fernando, D., Yu, T. Finite element modelling of debonding failures in steel beams flexurally strengthened with CFRP laminates. *Engineering Structures*, 2015, 86: pp. 213-224.